

Tetramer-aided sorting and single-cell RNA sequencing facilitate transcriptional profiling of antigen-specific CD8⁺ T cells

Kamalakaran Rajasekaran^{1,*}, Xiangnan Guan¹, Alireza Tafazzol, Habib Hamidi, Martine Darwish, Mahesh Yadav^{*}

Genentech, 1 DNA way, South San Francisco, CA 94080, USA

ARTICLE INFO

Keywords:

CMV pp65-specific CD8⁺ T cells
pMHC Tetramers
FACS sorting
Single-cell RNA sequencing
TCR analysis
Antigen-specific response gene signature
Cancer immunotherapy

ABSTRACT

Background: Recent advances in single-cell technologies and an improved understanding of tumor antigens have empowered researchers to investigate tumor antigen-specific CD8⁺ T cells at the single-cell level. Peptide-MHC I tetramers are often utilized to enrich antigen-specific CD8⁺ T cells, which however, introduces the undesired risk of altering their clonal distribution or their transcriptional state. This study addresses the feasibility of utilizing tetramers to enrich antigen-specific CD8⁺ T cells for single-cell analysis.

Methods: HLA-A*02:01-restricted human cytomegalovirus (CMV) pp65 peptide-specific CD8⁺ T cells were used as a model for analyzing antigen-specific CD8⁺ T cells. Single-cell RNA sequencing and TCR sequencing were performed to compare the frequency and gene expression profile of pp65-specific TCR clones between tetramer-sorted, unstimulated- and tetramer-stimulated total CD8⁺ T cells.

Results: The relative frequency of pp65-specific TCR clones and their transcriptional profile remained largely unchanged following tetramer-based sorting. In contrast, tetramer-mediated stimulation of CD8⁺ T cells resulted in significant gene expression changes in pp65-specific CD8⁺ T cells. An Antigen-Specific Response (ASR) gene signature was derived from tetramer-stimulated pp65-specific CD8⁺ T cells. The ASR signature had a predictive value and was significantly associated with progression free survival in lung cancer patients treated with anti-PD-L1, anti-VEGF, chemotherapy combination (NCT02366143). The predictive power of the ASR signature was independent of the conventional CD8 effector signature.

Conclusions: Our findings validate the approach of enriching antigen-specific CD8⁺ T cells through tetramer-aided Fluorescence-Activated Cell Sorting (FACS) sorting for single-cell analysis and also identifies an ASR gene signature that has value in predicting response to cancer immunotherapy.

Introduction

Antigen-specific CD8⁺ T cells play a pivotal role in mounting an acquired immune response against various pathogens and tumor cells. Enhanced recognition of tumor antigens by T cells is a key step in the reinvigoration of the immune system during the immune checkpoint blockade (ICB) therapy. In fact, many clinical approaches including cancer vaccines and adoptive T cell therapies rely on direct targeting of tumor antigen-specific T cells to improve on the existing efficacy with ICB therapy [1–5]. The tumor antigens recognized by T cells include tumor mutation-derived neoantigens, viral antigens, tumor-associated antigens or cancer testis antigens. Although it has been established that antigen encounter of T cells in the tumor profoundly alters the T cell

differentiation and activation status, a thorough investigation of antigen-specific T cell responses is lacking and the underlying mechanisms or biomarkers of antigen-specific response during ICB are not completely understood. Single-cell technologies have emerged as powerful tools to explore cellular heterogeneity at the resolution of individual cells and can be exploited to provide more accurate understanding of tumor-specific T cell response in cancer patients. With these approaches, it is possible to obtain both TCR clonal and transcriptional information that can reveal the phenotype and biomarkers of antigen-specific T cells during ICB therapy and provide mechanistic insights to predict responses. Specifically, monitoring antigen-specific T cell responses during immunotherapy in the peripheral blood is of interest since it could potentially provide a non-invasive method for

* Corresponding authors.

E-mail addresses: rajasek1@gene.com (K. Rajasekaran), yadavm2@gene.com (M. Yadav).

¹ Co-first authors.

assessing quality of anti-tumor response that could potentially be linked to predicting clinical benefit. Quantification of antigen-specific T-cell responses is often accomplished by the use of peptide/MHC complexes. These fluorochrome-conjugated peptide-loaded MHC I multimers such as tetramers, pentamers, dextramers are widely used to identify antigen-specific CD8⁺ T cells and to track tumor antigen-specific T cells [1,2,4,6].

Using peptide-loaded MHC-I tetramers to sort antigen-specific T cells facilitates integration of single-cell analysis to simultaneously assess clonal composition, phenotype, functionality and transcriptome of individual clones of interest [7–11]. More specifically, in tumor-reactive T cells, this approach facilitates evaluation of heterogeneity of antigen-specific responses, their TCR clonal distribution and transcriptional profile [8,10,12] or to track neoantigen-specific T cells to define transition from naive to an activated or effector state during cancer vaccine treatment [1].

One of the major concerns in using tetramers to characterize antigen-specific T cells at the single-cell level is the high affinity interaction of these peptide-loaded MHC I molecules with their cognate TCRs, which raises the possibility of tetramers activating the T cells during the sample preparation and sorting process. Under certain conditions, tetramer stimulation can lead to activation and proliferation of antigen-specific CD8⁺ T cells [12–14]. These previous studies highlight the importance of investigating if the use of tetramers for sorting antigen-specific T cells creates an unexpected change in cellular composition or transcriptional profile of the sorted antigen-specific CD8⁺ T cells.

In this study, we took advantage of a well-characterized HLA-A*02:01-restricted human cytomegalovirus (CMV) antigen, pp65 and used tetramer-based sorting to enrich pp65-specific CD8⁺ T cells from peripheral blood mononuclear cells (PBMCs) of HLA-A*02:01 positive healthy donors and single-cell RNA-seq with targeted V(D)J capture was performed. Our results indicate that the relative frequency of antigen-specific TCR clones and their transcriptional profile remain largely unaltered following tetramer-aided FACS sorting. In contrast, many genes associated with T cell activation were induced when pp65-specific CD8⁺ T cells were stimulated with tetramers under activating conditions. We used these data to derive a transcriptional gene signature of antigen-specific response (ASR) and interestingly, this gene signature was predictive of improved progression free survival (PFS) in chemotherapy-naive non-squamous non-small cell lung cancer (NSCLC) patients (NCT02366143) treated with anti-PD-L1 (atezolizumab) in combination with anti-VEGF (bevacizumab) and chemotherapy. Our study validates the approach of enriching antigen-specific CD8⁺ T cells through tetramer sorting for single-cell analysis and also identifies an antigen-specific response gene signature that correlates with response to cancer immunotherapy.

Materials and methods

Peripheral blood mononuclear cells from healthy donors

Leukopacks were obtained from two healthy volunteers who were previously analyzed and identified for the frequency of HLA-A*02:01-restricted CMV-pp65-specific precursor CD8⁺ T cells. PBMCs were isolated through Ficoll-Paque gradient centrifugation while following relevant guidelines and regulations. Healthy donor samples were utilized with IRB approval and obtained with written informed consent.

Viral peptides

HLA-A*02:01-restricted epitope from Cytomegalovirus pp65₄₉₅₋₅₀₃ (AS-28328, NLVPMVATV) and from influenza matrix protein, 58-66 (AS-28310, GILGFVFTL) with a purity of ≥95% was purchased from Anaspec.

Cell Staining and flow cytometry

Frozen PBMCs were thawed and washed using 1X CTL anti-aggregate wash solution (CTL-AA-005). Staining for flow cytometry was performed in MACS buffer (PBS pH 7.2, 0.5% BSA, 2mM EDTA). The CD8⁺ T cells were identified using cell surface markers, anti-CD3-BUV737 (BD, 612750) and anti-CD8-BUV395 (BD, 563795). Dead cells were excluded using Fixable Viability Dye eFluo780 (eBioscience, 65-0865-14). For analyzing activation-induced cytokine production, cells were permeabilized (BD, 554714) and stained with anti-IFN-γ (Biolegend, 502515) and anti-TNF-α (BD, 554514). Cells were analyzed using a BD Symphony FACS analyzer. Data was analyzed using FlowJo 10.7.1.

Spectral flow cytometry was performed to characterize CMVpp65-specific CD8⁺ T cells. PE- and APC-labeled HLA-A*02:01 tetramer loaded with CMV pp65₄₉₅₋₅₀₃ (NLVPMVATV) was synthesized internally utilizing the methodology described previously [15]. Total PBMCs were stained with anti-CD3 (PerCPCy5.5), anti-CD8 (BUV563), anti-CD27 (BV650), anti-CD45RA (BV570), anti-CD28 (BUV395), and anti-PD-1 (BUV737). Dead cells were stained using Zombie NIR viability dye and excluded from the analysis. Cells were analyzed using a Cytek Aurora spectral flow analyzer. Data was analyzed using FlowJo 10.7.1.

FACS sorting of total CD8 and CMV pp65-specific CD8⁺ T cells

CD8⁺ T cells were initially enriched from total PBMCs using CD8⁺ T cell isolation kit (Miltenyi Biotec, 130-096-495). From these negatively selected sample preparation, total CD8⁺ T cells were further enriched through FACS sorting. For sorting total CD8⁺ T cells, cells were stained with anti-CD3 and anti-CD8. To exclude dead cells, cells were also stained with Fixable Viability Dye eFluo780 (eBioscience, 65-0865-14). These highly enriched total CD8⁺ T cells were used for downstream single-cell analysis of total CD8⁺ T cells or tetramer-sorted pp65-specific CD8⁺ T cells. In order to sort CMV pp65-specific CD8⁺ T cells, in addition to the surface staining for CD3 and CD8, cells were also stained with PE- and APC-labeled HLA-A*02:01 tetramer loaded with CMV pp65₄₉₅₋₅₀₃. CD3⁺CD8⁺ T cells that were positively stained for both PE- and APC-labeled tetramers were considered pp65 peptide-specific and were sorted using a BD FACS Aria Fusion cell sorter. Sorted cells were collected in RPMI 1640 medium with FBS at a final concentration of 10%.

T cell activation assay

Following enrichment of total CD8⁺ T cells from PBMCs through negative selection, cells were stimulated with titrating concentrations of fluorochrome-unconjugated, HLA-A*02:01 tetramer loaded with CMV pp65₄₉₅₋₅₀₃. As a positive control, CD8⁺ T cells were also stimulated with PMA/Ionomycin (cell stimulation cocktail with protein transport inhibitors, 00-4975-93, ThermoFisher Scientific). rhIL-2 at a final concentration of 50U/ml was added in all the culture conditions included in the assay. Brefeldin A (BD GolgiPlug 555029) was added to the wells with CD8⁺ T cells stimulated with the tetramer during the last 8 h of incubation at a final concentration of 1:1000. Following 12 h of incubation, cells were harvested, and stained for cell surface markers and for intracellular IFN-γ and TNF-α. Dead cells were excluded from analysis using Fixable Viability Dye eFluo780 (eBioscience, 65-0865-14).

To prepare cells for single-cell RNA sequencing and TCR sequencing, negatively selected and FACS-sorted total CD8⁺ T cells were cultured for 12 h in regular RPMI medium supplied with 50U/ml of rhIL-2 or were stimulated with 5.0 ug/ml of fluorochrome-unconjugated HLA-A*02:01 tetramer loaded with CMV pp65₄₉₅₋₅₀₃. Following 12 h of incubation, pp65-specific CD8⁺ T cells were sorted using a portion of the unstimulated total CD8⁺ T cells following staining with fluorochrome-conjugated tetramers (**sample: Tetramer-sorted**) as described previously. Dead cells were excluded during sorting by performing relevant staining for dead cells. For the remaining unstimulated total CD8⁺ T

cells (sample: **Unstimulated total CD8+ T cells**) and for the tetramer-stimulated CD8+ T cells (sample: **Tetramer-stimulated total CD8+ T cells**), FACS sorting was performed to exclude dead cells.

Cytotoxicity assay

Two healthy donors with HLA-A*02:01 and a confirmed memory CD8+ T cell response to CMV were identified. Total CD8+ T cells from donor 1 and donor 2 enriched by negative selection on a magnetic column were used as effector cells in a cytotoxicity assay. Human B lymphoma cell line, C1R, transfected to express HLA-A*02:01 was used as a target. As a control, C1R cells transfected to express HLA-B*07:02 and parental C1R cells were also included in the assay. Parental and HLA-monoallelic C1R cell lines were pulsed with 2.5 µg/ml of HLA-A*02:01-restricted pp65 peptide (NLVPMVATV) overnight. The next day, target cells were washed and co-cultured with total CD8+ T cells that were maintained overnight in complete RPMI1640 medium with 50 U/ml of rIL-2. Effector cells were titrated to achieve different effector:target (E:T) ratio. A similar assay was also performed using FACS-sorted HLA-A*02:01-restricted CMV pp65-specific CD8+ T cells from donor 1 as effector cells and CMV pp65 peptide-pulsed (2.5 and 1.25 µg/ml) or influenza A, M1 peptide (GILGFVFTL)-pulsed (2.5 µg/ml) parental and HLA-monoallelic C1R cells as targets. Peptides were titrated during pulsing to achieve a final concentration of 2.5 and 1.25 µg/ml concentration. Co-cultures were set up with an E:T ratio of 5:1. Following 4 h of co-culture, cells were stained with anti-human CD8 to gate on effector cells and anti-human CD19 to gate on target cells. Effector cell-induced apoptosis of target cells was measured using Alexa Fluor 488-conjugated Annexin V and propidium Iodide (PI) staining (Dead cell Apoptosis kit, V13245). Levels of effector cell-mediated cytotoxicity were analyzed through flow cytometry on a BD Symphony FACS analyzer. Data was analyzed using FlowJo 10.7.1.

Results

Tetramer-aided FACS sorting enriches functionally efficient CMV pp65-specific CD8+ T cells

Spectral flow cytometry was performed to confirm the existence and frequency of CMV pp65-specific CD8+ T cells in the PBMCs of the two healthy donors. pp65-specific CD8+ T cells were found at a frequency of 5.88% and 3.58% among the CD8+ T cells of the two donors (Fig. 1A).

The pp65-specific CD8+ T cells predominantly lacked CD28 expression and showed a non-naive memory phenotype (Fig. 1A). In addition to an effector memory phenotype (CD27-CD45RA-), in donor 1, a good proportion was also found in the central memory (CD27+CD45RA-) phenotype, whereas in donor 2, they were found to have a TEMRA (CD27-CD45RA+) phenotype (Fig. 1A).

We next confirmed the functionality and specificity of pp65-specific CD8+ T from these two healthy donors. Co-culture of CD8+ T cells with pp65 peptide-pulsed HLA-A*02:01-expressing C1R cells showed killing of the target cells. This was evident only with C1R cells expressing HLA-A*02:01 but not with either HLA-B*07:02-expressing or parental C1R cells (Fig. 1B, C). The level of cytotoxicity was directly proportionate to the effector:target ratio (Fig. 1C). Next, we explored if this cytotoxicity of pp65-specific CD8+ T cells is maintained following tetramer-aided FACS sorting of antigen-specific CD8+ T cells. Cytotoxicity was observed with FACS-sorted pp65-specific CD8+ T cells from donor 1 against pp65 peptide-pulsed HLA-A*02:01-expressing C1R cells but not against either HLA-B*07:02-expressing or parental C1R cells (Fig. 1D). The sorted pp65-specific CD8+ T cells also exhibited minimal cytotoxicity against Flu M1 peptide-pulsed HLA-A*02:01-expressing C1R cells (Fig. 1E) indicating the specificity of the sorted CD8+ T cells in recognizing HLA-A*02:01-restricted CMV pp65 peptide. Taken together, these data suggested that tetramer-aided FACS sorting facilitated the enrichment of functional pp65-specific CD8+ T cells.

Tetramer sorting does not change the clonal distribution of antigen-specific CD8+ T cells

To investigate the impact of tetramer-aided FACS sorting on the clonal distribution and transcriptional profiles of antigen-specific T cells, we performed single-cell RNA-seq combined with TCR-seq using FACS-sorted CMV pp65-specific CD8+ T cells (sample: tetramer-sorted) or FACS-sorted unstimulated total CD8+ T cells (sample: unstimulated). Total CD8+ T cells stimulated with the tetramer under activating conditions (sample: tetramer-stimulated) were used as control to derive the gene expression profile of activated pp65-specific CD8+ T cells (Fig. 2).

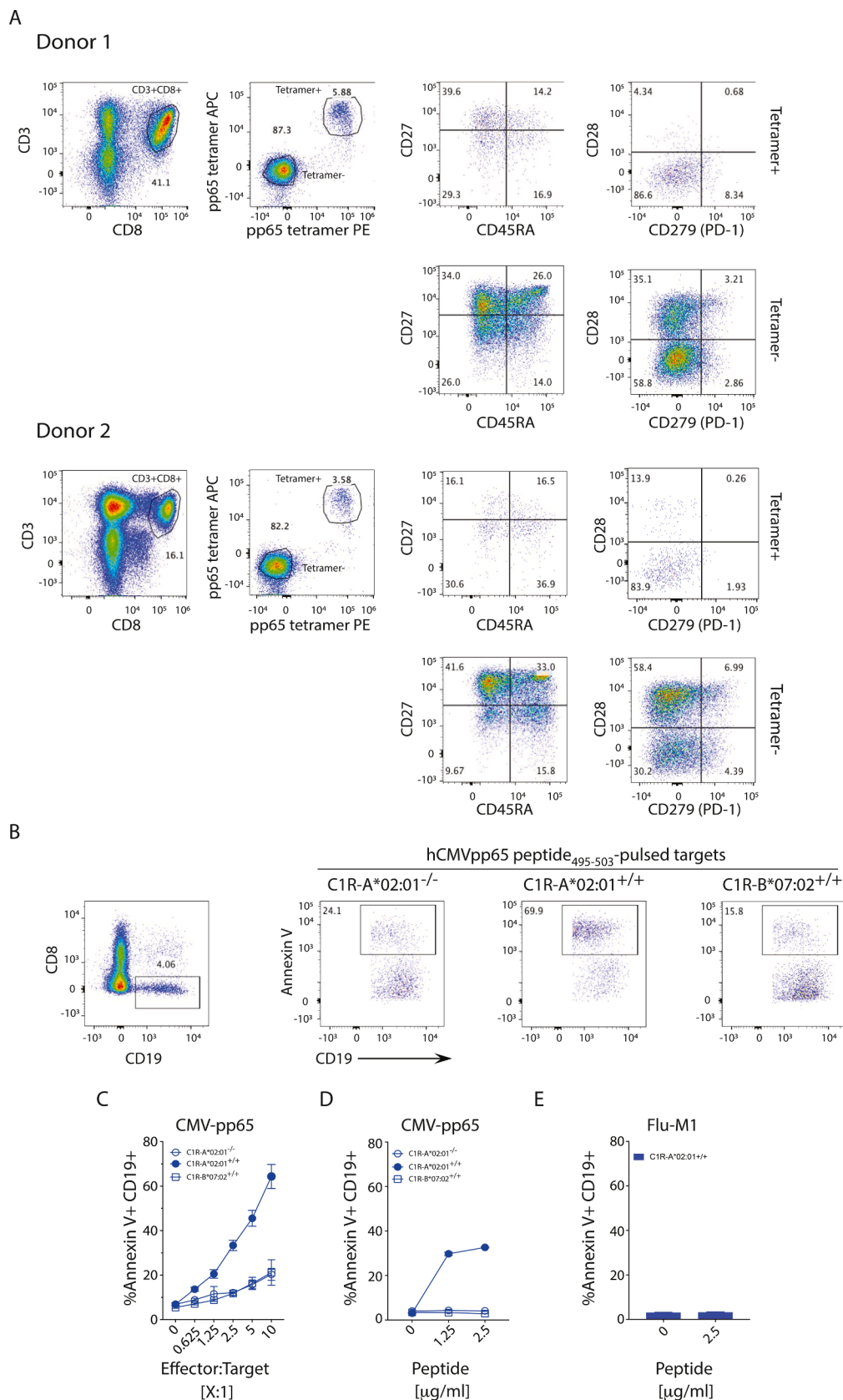
We used TCR clones from tetramer-sorted CD8+ T cells to derive a list of pp65 clonotypes and searched for them in the other two samples (unstimulated and tetramer-stimulated total CD8+ T cells). In the unstimulated total CD8+ T cells, the proportion of pp65-specific cells was determined to be 5.33% and 3.75% in donor 1 and donor 2, respectively, which aligned with the frequencies measured by FACS (5.88% and 3.58%, respectively, Fig. 1A). Furthermore, the distribution of top pp65-specific TCR clones detected was largely comparable (Fig. 3A, Supplemental Fig. 1A, Supplemental Tables 1, 2) between tetramer-sorted, unstimulated or tetramer-stimulated total CD8+ T cells. The higher proportion of the pp65-specific TCR clones in the tetramer-sorted sample reflected the enrichment of antigen-specific CD8+ T cells through tetramer-sorting.

Single-cell RNA-seq revealed the phenotypic subsets within antigen-specific CD8+ T cells

The integration of single-cell RNA-seq and TCR-seq as shown in Fig. 2 allowed the characterization of CD8+ T cells in a clone specific manner. In total, we sequenced 68,730 CD8+ T cells, of which 62,194 cells also had a mapped TCR sequence (90.49%). Unsupervised clustering revealed seven distinct CD8 T cell subtypes: naïve, central memory (CM), effector memory (EM), effector memory CD45RA+ (TEMRA), *IFNG* expressing cluster, *KLRC2* expressing cluster and mucosa-associated invariant T cells (MAIT) cluster (Supplemental Fig. 1B, C, Supplemental Table 3). Uniform manifold approximation and projection (UMAP) analysis showed a similar profile of T cells from both donors (Supplemental Fig. 1D). Enrichment of specific marker genes in different clusters is depicted in supplemental Fig. 1E. Tetramer-sorted, enriched CMV pp65-specific CD8+ T cells mainly displayed TEMRA and EM phenotypes (Supplemental Fig. 2A), which is similar to what was observed in FACS analysis (Fig. 1A). The unstimulated and tetramer-stimulated total CD8+ T cells were more widely distributed across different clusters (Supplemental Fig. 2A). These results were consistent with previous findings that CMV pp65-specific CD8+ T cells in the peripheral blood are predominantly of the late-differentiated effector memory (EM) and effector memory CD45RA+ (TEMRA) phenotypes [16,17].

Next, we analyzed the cellular composition and distribution of CMV pp65-specific CD8+ T cells in different samples from the two donors. As already depicted in supplemental Fig. 2A, in the tetramer-sorted sample, antigen-specific CD8+ T cells were largely found within the TEMRA and EM clusters in both donors (Fig. 3B). This was also evident when individual pp65-specific TCR clones were assessed for their phenotype (Fig. 3C). The cellular composition of pp65-specific CD8+ T cells remained largely unchanged when compared between the tetramer-sorted and the unstimulated total CD8+ T cells, except for a few less abundant TCR clones, generally associated with lower numbers of pp65-specific CD8+ T cells within the unstimulated total CD8+ T cells sample (Fig. 3C, Supplemental Tables 4, 5). Of note, the pp65-specific CD8+ T cells from the tetramer-stimulated samples were enriched within the *IFNG* cluster (Fig. 3B, C) indicating a state of activation. Similarly, FACS analysis showed induction of IFN-γ and TNF-α within a subset of CD8+ T cells activated with tetramer (Supplemental Fig. 2B), while PMA/Ionomycin stimulation resulted in IFN-γ and TNF-α production in a larger

Figure 1



(caption on next page)

Fig. 1. Detection of CMV pp65-specific CD8+ T cells and their phenotypic and functional analysis. (A) Tetramer-aided detection of CMV pp65-specific CD8+ T cells in the PBMCs and their phenotype. (B) Gating strategy to analyze cytotoxicity mediated by CD8+ T cells against peptide-pulsed (2.5 ug/ml) monoallelic C1R cell lines. Percentage of Annexin positive cells within the CD19+ cells was considered for analysis. (C) Cumulative analysis of cytotoxicity against CMV pp65 peptide-pulsed (2.5 ug/ml) C1R parental or monoallelic cell lines as measured by %Annexin V+CD19+ cells following coculture with total CD8+ T cells from donor 1 and donor 2. Effector:Target ratio indicates the proportion of effector cells (CD8+ T cells) in culture with respect to 50000 target cells. (D) Analysis of cytotoxicity against CMV pp65 peptide-pulsed C1R parental or monoallelic cell lines as measured by %Annexin V+CD19+ cells following coculture with tetramer-aided FACS-sorted CMVpp65-specific CD8+ T cells from donor 1. C1R target cells were pulsed with 2.5 ug/ml or 1.25 ug/ml of CMV pp65 peptide. Effector:Target ratio was at 5:1. (E) Analysis of cytotoxicity against Flu M1 peptide-pulsed (2.5 ug/ml) HLA-A*02:01-expressing C1R monoallelic cell line as measured by %Annexin V+CD19+ cells following coculture with tetramer-aided FACS-sorted CMVpp65-specific CD8+ T cells from donor 1. Cytotoxicity against peptide-unpulsed target cells is also shown as control in C, D and E.

proportion of CD8+ T cells in both donors (Data not shown).

It was noteworthy that some of the clones observed in the tetramer-sorted sample were not represented in the unstimulated sample (Fig. 3C, Supplemental Fig. 1A), which could be attributed to the enrichment of pp65-specific CD8+ T cells in the tetramer-sorted sample.

These data indicate that tetramer sorting did not alter the composition of pp65 antigen-specific CD8+ T cells whereas tetramer stimulation promoted the transition to the *IFNG* phenotype.

Tetramer sorting does not alter antigen-specific CD8+ T cell transcriptome

Next, we tested if the interaction of tetramers with the TCR during the sample preparation and sorting process impacted the transcriptome of the antigen-specific CD8+ T cells. Differential gene expression analysis was performed comparing pp65-specific CD8+ T cells from the tetramer-sorted samples with pp65-specific CD8+ T cells from the unstimulated total CD8+ T cells samples (Supplemental Table 6). As shown in Fig. 4A, a minimal number of differentially expressed genes (DEGs) mostly unrelated to T cell activation except *GPLY*, *XCL1* and *LGALS1*, were modestly upregulated in the tetramer-sorted sample. On the other hand, *EOMES* was found to be modestly downregulated in the pp65-specific CD8+ T cells from the tetramer-sorted sample (Fig. 4A).

In contrast, when comparing the gene expression profile of pp65-specific CD8+ T cells from tetramer-sorted samples with those from tetramer-stimulated samples (Supplemental Table 7), 906 genes were up-regulated and 599 genes were down-regulated in the tetramer-stimulated condition (Fig. 4B). Many of the top up-regulated genes were associated with T cell effector functions downstream of TCR activation such as *IFNG*, *TNF*, *CCL3*, *CCL4*, *XCL1*, *XCL2*, *IL2RA* (CD25), *TNFRSF9* (4-1BB, CD137), and *TNFRSF1B* (Fig. 4B, Supplemental Table 7). In addition, genes associated with antigen recognition such as *CD82*, *CD160* and *CRTAM* were also found to be upregulated following tetramer-mediated activation. An almost similar pattern of gene expression changes was observed when comparing pp65-specific CD8+ T cells in the tetramer-stimulated samples with those from the unstimulated total CD8+ T cells (Supplemental Fig. 2C, Supplemental Table 8). Tetramer-mediated activation and resultant transcriptional changes were restricted to the pp65-specific CD8+ T cells. No significant transcriptional changes were observed when comparing non-pp65-specific CD8+ T cells from tetramer-stimulated samples with those from unstimulated samples (Supplemental Fig. 2D, Supplemental Table 9).

We extended this differential gene expression (DGE) analysis to individual pp65-specific TCR clones in the two donors. Towards this, we compared the gene expression profiles of TCR clones that had at least 10 cells in all three samples. DGE analysis at the level of individual TCR clones reiterated our findings that tetramer sorting did not have a profound impact on the gene expression profile of pp65-specific CD8+ T cells. Further, in each of the clones tested, genes associated with T cell effector functions were consistently upregulated in the tetramer-stimulated condition compared to the tetramer-sorted condition (Supplemental Figs. 3 and 4).

Taken together, our findings confirmed that while tetramers had the capacity to activate T cells in an antigen-specific manner, short term exposure to tetramers during the staining and sorting process did not

result in significant alteration of the transcriptional profile of antigen-specific CD8+ T cells.

Tetramer-mediated activation resulted in consistent transcriptional changes within pp65-specific TCR clones

DGE analysis was performed either on bulk or individual pp65-specific TCR clones. To objectively compare and identify genes associated with activation in individual pp65-specific CD8+ T cell clones, we compared gene signatures of pp65-specific TCR clones that had at least 10 cells in all three samples (Fig. 4C, Supplemental Tables 10, 11). As depicted in Fig. 4C, in the cytotoxicity signature, expression of *GZMB*, *PRF1* and *CRTAM* (class I-restricted T cell-associated molecule) were consistently upregulated within TCR clones in the tetramer-stimulated condition. Expression of the other granzymes such as *GZMA*, *GZMH*, *GZMK* and *granulysin (GNLY)* were downregulated following tetramer-mediated activation of pp65-specific CD8+ T cells.

In the gene signature for cytokines/chemokines, while *CCL4*, *IFNG* and *TNF* were upregulated, *CCL5* was downregulated following tetramer-mediated activation. The most consistently upregulated costimulatory receptor in the pp65-specific TCR clones following tetramer-mediated activation was *TNFRSF9* (CD137, 4-1BB) in addition to checkpoint receptors *LAG3* and *TIGIT*. Interestingly, *PDCD1* (PD-1) and *HAVCR2* (TIM3) showed stronger induction in the pp65-specific CD8+ T cells in donor 2 compared to donor 1 following tetramer-mediated activation. While the transcription factors *ZEB2*, *HIF1A*, *ID2* and *HOPX* were upregulated following tetramer-mediated activation, transcription factors *TBX21* and *EOMES* were downregulated.

An 'Antigen-Specific Response' (ASR) gene signature was derived using the upregulated genes in tetramer-stimulated compared to tetramer-sorted pp65-specific CD8+ T cells. The ASR gene signature consisted of top 21 genes that were upregulated in the pp65-specific CD8+ T cells in the tetramer-stimulated condition compared to the tetramer-sorted condition. Along with *CD8A*, in addition to genes associated with T cell activation and effector functions such as *IFNG*, *TNF*, *CCL3*, *CCL4*, *TNFRSF9*, *IL2RA*, the ASR gene signature also contained genes associated with antigen recognition (*CD82*, *CRTAM*, *CD160*), and metabolic regulation such as *PGAM1*, *PKM* and *FABP5*. The most consistent upregulation among the different pp65-specific TCR clones in donor 1 and donor 2 was observed in the ASR gene signature in the 'tetramer-stimulated' condition. DGE analysis at the level of individual clones confirmed that genes associated with the ASR gene signature were consistently upregulated following tetramer-mediated stimulation across individual clones (Supplemental Figs. 3 and 4). Thus, enrichment of antigen-specific CD8+ T cells through tetramer-aided FACS sorting facilitated comparison of gene signatures at the level of individual TCR clones.

ASR gene signature is associated with better clinical outcome in cancer immunotherapy

To explore if ASR signature derived from activated pp65-specific T cells can be used as a surrogate for antigen-specific T cell response in the tumor milieu, and predict response to immunotherapy, we applied ASR signature in lung cancer patients treated with ICB and chemotherapy

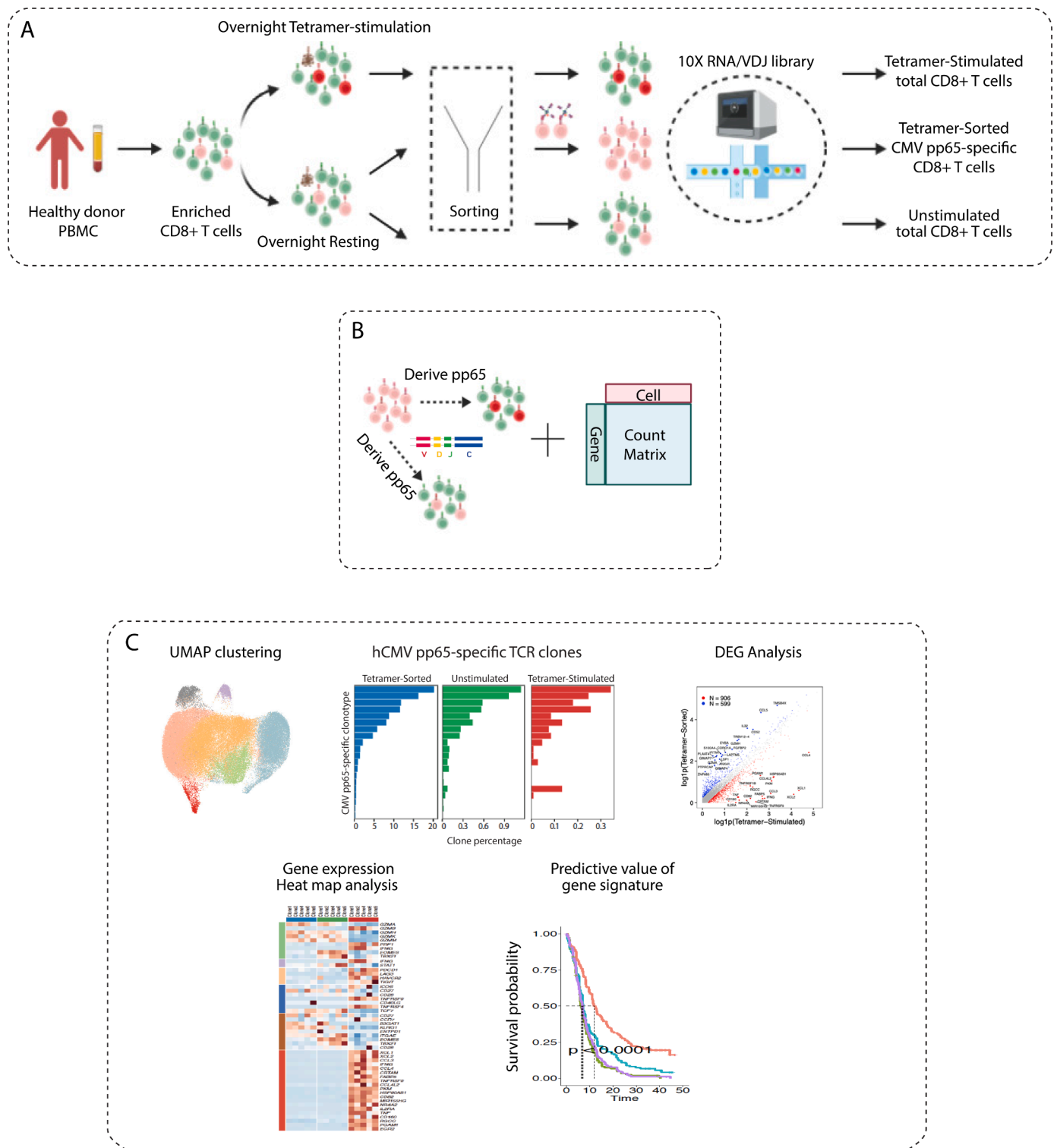


Fig. 2. Schematic representation of the workflow for sample processing and preparation for single-cell RNA sequencing and analysis. (A) Total CD8+ T cells enriched from healthy donor PBMCs were either left unstimulated or were stimulated with 5 ug/ml of the same tetramers used for sorting but were not conjugated to fluorochromes. Following overnight culture, a portion of the unstimulated total CD8+ T cells were used to sort live, antigen-specific CD8+ T cells using HLA-A*02:01-restricted CMV pp65 peptide-loaded, fluorochrome-conjugated tetramers. In addition, live total CD8+ T cells were also FACS-sorted from the unstimulated and tetramer-stimulated conditions. (B) Derivation of pp65-specific TCR clones and integration with gene expression data. The unstimulated tetramer-sorted antigen-specific CD8+ T cells were used to derive the pp65-specific TCR clones, which were used to nominate pp65-specific clones in the unstimulated total CD8+ T cells and tetramer-stimulated total CD8+ T cells (C) Following Seurat-based cell clustering, pp65-specific clone distribution and differentially expressed genes were compared. In addition, an ‘Antigen-Specific Response’ gene signature was derived and its predictive value in cancer immunotherapy tested.

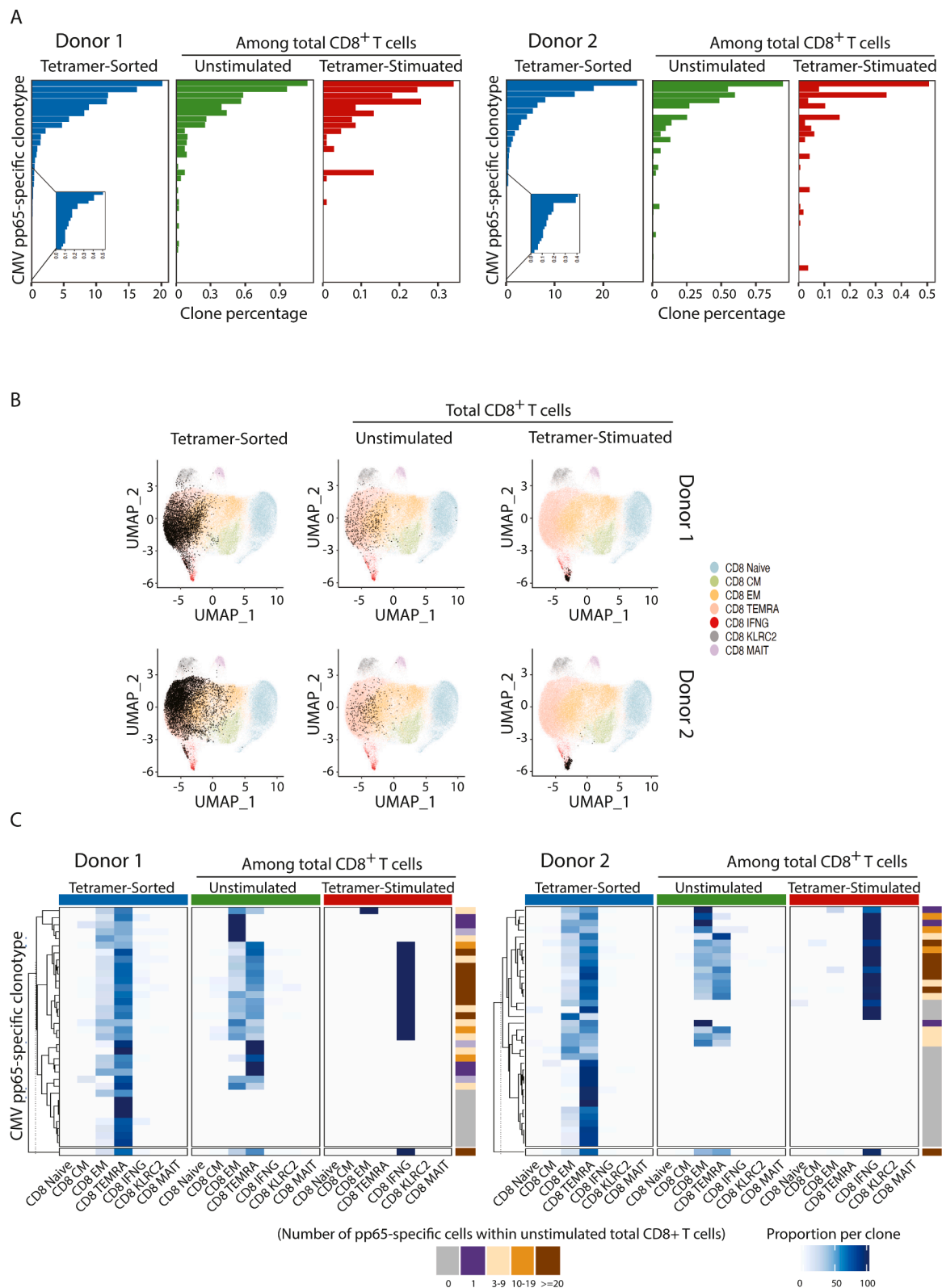


Fig. 3. Analysis of CMVpp65-specific CD8⁺ TCR clones in the different sample preparations. (A) Bar diagram represents the proportion of corresponding pp65-specific TCR clones identified in the tetramer-sorted, unstimulated and tetramer-stimulated total CD8⁺ T cell samples. Proportions were calculated for each TCR clone out of the total CD8⁺ T cells in that sample. The graph in the inset indicates clones identified at lower frequency in the tetramer-sorted sample. (B) Localization of CMV pp65-specific CD8⁺ T cells within CD8⁺ T cell clusters in the different samples. Upper panel depicts pp65-specific CD8⁺ T cells from donor 1 and the lower panel represents pp65-specific CD8⁺ T cells from donor 2. The black dots are individual CD8⁺ T cells with pp65-specific TCR. (C) Intensity plot depicting the distribution of each pp65-specific TCR clone in the different CD8⁺ T cell clusters in the different samples in donor 1 (Left panel) and donor 2 (Right panel). Each row represents a single pp65-specific TCR clone. The abundance (number of pp65-specific cells) of each pp65-specific CD8⁺ TCR clone in the unstimulated total CD8⁺ T cells is also depicted on the right side.

combination (NCT02366143). This study showed that addition of atezolizumab to bevacizumab plus chemotherapy significantly improved progression free survival and overall survival among patients with metastatic non squamous non-small lung cancer (NSCLC) [18]. ASR gene signature was predictive of better progression free survival in NSCLC patients treated with atezolizumab in combination with bevacizumab, carboplatin and paclitaxel but not in the bevacizumab, carboplatin and paclitaxel group (Fig. 4D log-rank p value < 0.0001 , Supplemental Table 12). In the univariate analysis, ASR high patients had significantly better outcome (PFS) in the atezolizumab containing arm (Table 1: HR = 0.55, 95% CI = 0.43-0.71, $p = 2.82e-06$) but not in the control arm (Table 1: HR = 1.07, 95% CI = 0.83 to 1.35, $p = 0.51$). A previously described CD8 effector gene signature [19] (*CD3E*, *CD8A*, *CXCL10*, *CXCL9*, *EOMES*, *GZMA*, *GZMB*, *IFNG*, *KLRD1*, *NKG7*, *PRF1*, *TBX21*) modified to include additional effector genes was also tested for its predictive value. The overlapping and unique genes that comprise the ASR gene signature and CD8 effector gene signature are depicted in supplemental Fig. 5A. CD8 effector gene signature was also associated with significantly better outcome (PFS) in the atezolizumab arm (Supplemental Fig. 5B, log-rank p value < 0.0001 , Supplemental Table 12). We assessed how much of the effect of the ASR signature could be explained by the CD8 effector signature by testing ASR signature in a multivariate model with the CD8 gene signature using Cox proportional hazards regression model. ASR high patients still performed significantly better in Atezo containing arm (Table 1: HR = 0.62, 95% CI = 0.45 to 0.9, $p = 0.01$) when adjusting for the CD8 effector gene signature whereas most of the observed predictive value of the CD8 gene signature were not maintained when adjusting for the ASR gene signature (Table 1: HR = 0.83, 95% CI = 0.58 to 1.13, NS). This suggested a predictive value for the ASR signature that is independent of the CD8 effector signature in tumor immunotherapy clinical trials. To understand the differences in these two signatures, survival outcomes (PFS) were compared taking into consideration the expression of these two signatures (Supplemental Fig. 5C, D). In the atezolizumab arm, approximately 21% of patients are discordant for the median cutoff (i.e., when they are high for ASR gene signature, they are low for CD8 effector gene signature and vice versa). Patients with tumors that had ASR low and CD8 effector high gene signatures have significantly worse outcomes than patients with tumors that had ASR high and CD8 effector high gene signatures [PFS HR 2.6 (95% CI, 1.51-4.5); $p < 0.001$]. Interestingly, patients with tumors that had ASR high and CD8 effector low gene signatures had similar outcomes to immunotherapy as those with ASR high and CD8 effector high gene signatures [PFS HR 1.6 (95% CI, 0.91-2.8; $p = 0.099$)]. Though there was an increase in the hazard

ratio, this was not statistically significant. These findings imply that the ASR gene signature may have an added value compared to CD8 effector gene signature in predicting the outcome of atezolizumab-mediated immunotherapy.

Discussion

With the recent focus on neoantigens in cancer immunotherapy and technological advances in single-cell sequencing approaches, there is an increased interest in understanding antigen-specific T cell responses in cancer patients. Many of these approaches utilize pMHC tetramers to identify and isolate antigen-specific T cells for downstream single-cell analysis. However, the underlying issue of whether such processing of T cells leads to alterations in cellular composition or transcriptional profile has not been thoroughly investigated.

We addressed this using the well-established model of CMV pp65-specific CD8+ T cells. Our findings revealed that following tetramer-aided FACS sorting, the relative frequency of the pp65-specific TCR clones remained largely intact when compared to their counterparts within total CD8+ T cells. In addition, this approach enabled enrichment of pp65-specific CD8+ T cells whereby clones that were present at lower frequency which were barely detectable within the total CD8+ T cells were now detected.

Cell clustering analysis confirmed that pp65-specific CD8+ T cells were predominantly of the TEM or TEMRA phenotype. These results were consistent with previous findings that CMV pp65-specific CD8+ T cells in the peripheral blood are predominantly of the late-differentiated effector memory (EM) and effector memory CD45RA+ (TEMRA) phenotypes [16,17]. Tetramer-aided FACS sorting did not have an impact on this phenotype distribution in individual TCR clones, which further confirmed that this approach does not alter the clonal representation of antigen-specific CD8+ T cells but rather enriches the frequency of specific TCR clones.

In addition to tetramer-aided FACS sorting, CD8+ T cells from the same donors stimulated with the tetramers under activating conditions allowed us to study the transcriptional profile of activated pp65-specific CD8+ T cells. This analysis revealed that while the tetramers had the ability to activate CD8+ T cells when exposed long term under activating conditions, the duration of exposure during the process of labeling and sorting had minimal impact on the transcriptional profile. There were a few genes such as *TBX21* and *EOMES*, which were sensitive to this process and might exhibit subtle changes in their expression. However, the level of concordance observed in the gene signatures from the pp65-specific CD8+ T cells in the tetramer-sorted and unstimulated total CD8+ T cells strongly supports the approach of enriching antigen-specific CD8+ T cells.

The ASR gene signature derived from the tetramer-stimulated pp65-specific CD8+ T cells closely resembled markers of virus-responsive CD8+ T cells from a previous study that aimed at identifying rare antigen-responsive cells from within unselected populations of T cells [20]. Their study further revealed that the candidate marker genes of virus-responsive CD8+ T cells were not analogous to those of autoantigen-reactive CD8+ T cells. While the similarities or differences in the characteristics of autoantigen-reactive and tumor antigen-reactive CD8+ T cells need further exploration, several studies have highlighted the phenotypic and functional resemblance of virus-specific and tumor antigen-specific CD8+ T cells [10,21]. In fact, tumor-reactive T cells have been shown to respond to tumor antigens in a similar fashion to viral-specific T cells during chronic infection with expression of high levels of inhibitory molecules such as PD-1, CTLA-4, and LAG-3 and impaired production of effector cytokines including IFN- γ , TNF- α , and IL-2 [10,22-25]. The concept of stem-like CD8+ T cells giving rise to transitory effector-like CD8+ T cell population in a chronic LCMV infection model [26] was recapitulated in the human tumor study showing maintenance of stem-like CD8+ T cells in an intra-tumoral niche was critical for mounting an efficient anti-tumor immune

Table 1

Univariate and multivariate analyses of the predictive relevance of the ASR and CD8 Effector gene signature.

Signature	Median	N	Univariate HR (95% CI for HR)	p -value	Multivariate HR (95% CI for HR)	p - value
Atezo.carb.pac.bev						
ASR	Low	148				
	High	156	0.55 (0.43-0.71)	2.82E-06	0.62 (0.45-0.90)	0.01
CD8 Eff	Low	153				
	High	151	0.59 (0.48-0.77)	4.55E-05	0.83(0.59-1.14)	0.21
carb.pac.bev						
ASR	Low	171				
	High	153	1.07(0.83-1.35)	0.51	1.12 (0.83-1.49)	0.43
CD8 Eff	Low	160				
	High	164	1.01(0.83-1.2)	0.96	0.93(0.71-1.25)	0.64

Multivariable analysis using Cox proportional hazards regression model. HR: Hazard ratio, CI: Confidence interval.

response [27].

The ASR gene signature derived from viral antigen-specific CD8+ T cells from healthy donors responding to specific antigenic stimulation consisted of genes associated with antigen recognition and metabolic regulation in addition to conventional T effector function. This ASR gene signature might inform about the transcriptional changes in tumor antigen-reactive CD8+ T cells upon antigen recognition. This hypothesis is supported further by our observation that the ASR gene signature derived from tetramer-stimulated pp65-specific CD8+ T cells had a predictive value in the anti-PD-L1 treated lung cancer patients. While we examined the predictive value of the ASR gene signature using baseline tumor gene expression data, a further extension of this analysis would be to analyze ASR signature using gene expression data derived from on-treatment tumor biopsies or even applying it on the peripheral blood immune cells prior to treatment.

One of the limitations of our study was that we had restricted our analysis to CMV pp65-specific CD8+ T cells. Although we sought to extend the learnings to tumor antigen-specific CD8+ T cells, multiple factors such as the complicated process of identifying and detecting tumor antigen-specific T cells, scarcity of human cancer patient samples and the heterogeneity across patients, which may create another layer of complexity led us to use a viral antigen model. While a single tetramer was used in this analysis, the value of this approach needs to be investigated when more than one tetramer is used to enrich CD8+ T cells with different antigen specificities. Further, ASR gene signature was derived from the tetramer-stimulated pp65-specific CD8+ T cells. The similarities and dissimilarities of this signature with other virus-responsive and tumor antigen-responsive CD8+ T cells need to be analyzed. In one of the previous studies mentioned earlier [20], there was a close similarity in the identified markers of flu M1- and CMV pp65- responsive CD8+ T cells suggesting similarity across genes of virus-responsive CD8+ T cells. However, this signature needs to be tested against tumor antigen-reactive CD8+ T cells and further analysis is required to understand if ASR gene signature from our study overlaps with neoantigen-specific CD8+ T cell-centric gene signature.

Taken together, our findings provide a basis for analyzing tetramer-sorted tumor antigen-specific T cells at single-cell level whereby, performing single-cell RNA sequencing and TCR sequencing facilitates capturing the transcriptional profile of antigen-specific CD8+ T cells at the level of individual TCR clones. The ASR gene signature can be applied to cancer patients where antigen-specific T cell data is unavailable or acquiring this data is not possible. This signature may have utility in identifying tumor antigen-specific TCRs, which could even have implications for TCR-based T cell therapies.

Ethics approval

Healthy donor samples were utilized with IRB approval and obtained with written informed consent. NCT02366143 was a phase 3 clinical trial performed according to the Good Clinical Practice guidelines and the Declaration of Helsinki, with study protocol approval provided by independent ethics committees at each of the participating sites [18].

Availability of data and materials

The data sets that support the conclusions of this article are included within the article and its additional files. Data that supports the findings of this study are available from the corresponding authors upon reasonable request.

Funding

This study was funded by Genentech, Inc., a member of the Roche group.

CRedit authorship contribution statement

Kamalakaran Rajasekaran: Conceptualization, Methodology, Formal analysis, Investigation, Writing – original draft, Writing – review & editing, Resources. **Xiangnan Guan:** Validation, Formal analysis, Data curation, Writing – review & editing. **Alireza Tafazzol:** Writing – review & editing. **Habib Hamidi:** Formal analysis, Writing – review & editing. **Martine Darwish:** Methodology, Writing – review & editing. **Mahesh Yadav:** Conceptualization, Methodology, Supervision, Writing – review & editing.

Declaration of Competing Interest

The authors declare the following financial interests/personal relationships which may be considered as potential competing interests: All the authors are employees and stockholders of Genentech/Roche.

Acknowledgment

We would like to thank Ck Poon, Leesun Kim, Jiun Chiun Chang, Craig Blanchette and Magge Zepeda (Genentech) for their support in conducting this study.

Supplementary materials

Supplementary material associated with this article can be found, in the online version, at [doi:10.1016/j.tranon.2022.101559](https://doi.org/10.1016/j.tranon.2022.101559).

References

- [1] Z. Hu, et al., Personal neoantigen vaccines induce persistent memory T cell responses and epitope spreading in patients with melanoma, *Nat. Med.* 27 (3) (2021) 515–525.
- [2] N. van Rooij, et al., Tumor exome analysis reveals neoantigen-specific T-cell reactivity in an ipilimumab-responsive melanoma, *J. Clin. Oncol.* 31 (32) (2013) e439–e442.
- [3] N.A. Rizvi, et al., Cancer immunology. Mutational landscape determines sensitivity to PD-1 blockade in non-small cell lung cancer, *Science* 348 (6230) (2015) 124–128.
- [4] M. Pehlings, et al., Late-differentiated effector neoantigen-specific CD8+ T cells are enriched in peripheral blood of non-small cell lung carcinoma patients responding to atezolizumab treatment, *J. Immunother. Cancer* 7 (1) (2019) 249.
- [5] J.S. Holm, et al., Neoantigen-specific CD8 T cell responses in the peripheral blood following PD-L1 blockade might predict therapy outcome in metastatic urothelial carcinoma, *Nat. Commun.* 13 (1) (2022) 1935.
- [6] S. Krishna, et al., Stem-like CD8 T cells mediate response of adoptive cell immunotherapy against human cancer, *Science* 370 (6522) (2020) 1328–1334.
- [7] K.Y. Ma, et al., High-throughput and high-dimensional single-cell analysis of antigen-specific CD8(+) T cells, *Nat. Immunol.* 22 (12) (2021) 1590–1598.
- [8] A. Magen, et al., Single-cell profiling defines transcriptomic signatures specific to tumor-reactive versus virus-responsive CD4(+) T cells, *Cell Rep.* 29 (10) (2019) 3019–3032, e6.
- [9] T.S. Meldgaard, et al., Single-cell analysis of antigen-specific CD8+ T-cell transcripts reveals profiles specific to mRNA or adjuvanted protein vaccines, *Front. Immunol.* 12 (2021), 757151.
- [10] B.C. Miller, et al., Subsets of exhausted CD8(+) T cells differentially mediate tumor control and respond to checkpoint blockade, *Nat. Immunol.* 20 (3) (2019) 326–336.
- [11] Y. Yao, et al., Differential expression profile of gluten-specific T cells identified by single-cell RNA-seq, *PLoS One* 16 (10) (2021), e0258029.
- [12] S. Peng, et al., Sensitive detection and analysis of neoantigen-specific T cell populations from tumors and blood, *Cell Rep.* 28 (10) (2019) 2728–2738, e7.
- [13] R. Maile, et al., Antigen-specific modulation of an immune response by *in vivo* administration of soluble MHC class I tetramers, *J. Immunol.* 167 (7) (2001) 3708–3714.
- [14] B. Wang, et al., Naive CD8+ T cells do not require costimulation for proliferation and differentiation into cytotoxic effector cells, *J. Immunol.* 164 (3) (2000) 1216–1222.
- [15] B. Rodenko, et al., Generation of peptide-MHC class I complexes through UV-mediated ligand exchange, *Nat. Protoc.* 1 (3) (2006) 1120–1132.
- [16] E. Derhovanessian, et al., Infection with cytomegalovirus but not herpes simplex virus induces the accumulation of late-differentiated CD4+ and CD8+ T-cells in humans, *J. Gen. Virol.* 92 (Pt 12) (2011) 2746–2756.
- [17] M.L. Pita-Lopez, et al., Effect of ageing on CMV-specific CD8 T cells from CMV seropositive healthy donors, *Immun. Ageing* 6 (2009) 11.
- [18] M.A. Socinski, et al., Atezolizumab for first-line treatment of metastatic nonsquamous NSCLC, *N. Engl. J. Med.* 378 (24) (2018) 2288–2301.

- [19] Mariathasan, et al., TGF β attenuates tumour response to PD-L1 blockade by contributing to exclusion of T cells, *Nature* 554 (7693) (2018) 544–548.
- [20] Y.F. Fuchs, et al., Gene expression-based identification of antigen-responsive CD8(+) T cells on a single-cell level, *Front. Immunol.* 10 (2019) 2568.
- [21] L.M. McLane, M.S. Abdel-Hakeem, E.J. Wherry, CD8 T cell exhaustion during chronic viral infection and cancer, *Annu. Rev. Immunol.* 37 (2019) 457–495.
- [22] J. Fourcade, et al., Upregulation of Tim-3 and PD-1 expression is associated with tumor antigen-specific CD8+ T cell dysfunction in melanoma patients, *J. Exp. Med.* 207 (10) (2010) 2175–2186.
- [23] J. Matsuzaki, et al., Tumor-infiltrating NY-ESO-1-specific CD8+ T cells are negatively regulated by LAG-3 and PD-1 in human ovarian cancer, *Proc. Natl. Acad. Sci. U. S. A.* 107 (17) (2010) 7875–7880.
- [24] Y. Zhang, et al., Programmed death-1 upregulation is correlated with dysfunction of tumor-infiltrating CD8+ T lymphocytes in human non-small cell lung cancer, *Cell Mol. Immunol.* 7 (5) (2010) 389–395.
- [25] D.L. Barber, et al., Restoring function in exhausted CD8 T cells during chronic viral infection, *Nature* 439 (7077) (2006) 682–687.
- [26] W.H. Hudson, et al., Proliferating transitory T cells with an effector-like transcriptional signature emerge from PD-1(+) stem-like CD8(+) T cells during chronic infection, *Immunity* 51 (6) (2019) 1043–1058, e4.
- [27] C.S. Jansen, et al., An intra-tumoral niche maintains and differentiates stem-like CD8 T cells, *Nature* 576 (7787) (2019) 465–470.